Metabolomic Profiling of Anionic Metabolites in Head and Neck Cancer Cells by Capillary Ion Chromatography with Orbitrap Mass Spectrometry

ARTICLE *in* ANALYTICAL CHEMISTRY · APRIL 2014

Impact Factor: 5.64 · DOI: 10.1021/ac500951v · Source: PubMed

analytical chemistry

Article

pubs.acs.org/ac

Metabolomic Profiling of Anionic Metabolites in Head and Neck Cancer Cells by Capillary Ion Chromatography with Orbitrap Mass Spectrometry

Junhua Wang,[†] Terri T. Christison,[†] Kaori Misuno,[‡] Linda Lopez,[†] Andreas F. Huhmer,[†] Yingying Huang,*[,†] and Shen Hu*[,‡]

[†]Thermo Fisher Scientific, Inc., 355 River Oaks Parkway, San Jose, California 95134, United States

[‡]School of Dentistry and Jonsson Comprehensive Cancer Center, University of California, Los Angeles, 10833 Le Conte Avenue, Los Angeles, California 90095, United States

Supporting Information

ABSTRACT: A highly sensitive platform coupling capillary ion chromatography (Cap IC) with Q Exactive mass spectrometer has been developed for metabolic profiling of head and neck squamous cell carcinoma (HNSCC) cells. The Cap IC allowed an excellent separation of anionic polar metabolites, and the sensitivities increased by up to 100-fold compared to reversed-phase liquid chromatography and hydrophilic interaction chromatography performed at either high- or capillary-flow rates. The detection limits for a panel of standard metabolites were between 0.04 to 0.5 nmol/L (0.2 to 3.4 fmol) at a signal-to-noise ratio of 3. This platform was applied to an untargeted metabolomic analysis of head and neck cancer cells and stem-like cancer cells. Differential metabolomics analysis identified significant changes in energy metabolism pathways (e.g., glycolysis and tricarboxylic acid cycle). These experiments demonstrate Cap IC/MS as a powerful metabolomics tool by providing enhanced separation and sensitivity of polar metabolites combined with high resolution and accurate mass measurement (HR/AM) capabilities to differentiate isobaric metabolites.

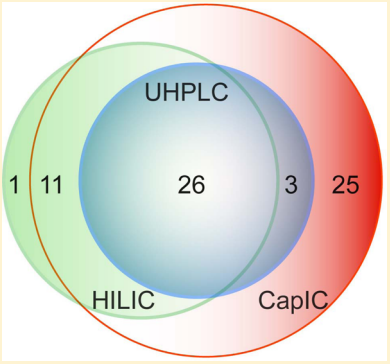

Metabolites represent an extremely diverse range of small molecules serving as substrates and products in cellular reactions. The fields of untargeted metabolomics attempt to quantify and pathway-map the vast array of metabolites present in a biological subject, which may provide novel insights into the biological phenotypes.[1,2] The general problems encountered when characterizing the metabolome are the highly complex nature and the wide concentration dynamic range of the compounds. Separation science plays an important role in metabolomics[3,4] by alleviating the sample complexity to achieve a comprehensive profiling analysis.[5−7] The strength of mass spectrometry (MS)-based metabolomics is best realized when coupled to a separation technique, such as capillary electrophoresis,[8−10] gas chromatography (GC),[11,12] or liquid chromatography (LC).[13] In the past decade, LC/MS-based analysis has evolved to the forefront because of its ability to analyze and identify a wide range of underivatized and thermally labile metabolites.[14,15] However, ionic and very polar compounds are unable to be retained on a conventional reversed-phase (RP) column. Recently, an ion-pairing LC (IPLC) method has been demonstrated by introducing certain ion-pairing agents e.g., diamyl ammonium[16] or tributylamine[17] to improve chromatographic retention for polar molecules. On the other hand, the hydrophilic interaction chromatography (HILIC) method has emerged as an alternative to RPLC and shows promise in separating polar compounds.[18,19] HILIC's retention of those polar compounds and use of solvents readily compatible with mass spectrometry have obtained increasing adoption in studies of complex aqueous metabolomes. However, a limitation of IPLC and HILIC methods lies in the sensitivity loss caused by high background interference to MS measurement.

Ion chromatography (IC) or ion-exchange chromatography offers an excellent complementary platform for separation of charged and polar compounds.[20] IC without suppression has been extensively applied to analysis of environmental, pharmaceutical, food, and beverage samples for chemical identity confirmation and trace-level analysis in complex matrices.[21,22] However, the analytical technique has majorly remained associated with analysis of small inorganic ions.[23,24] The coupling of IC with MS has been more successful thanks to the recent development of eluent suppression technology that allows continuous online desalting and conversion of high-salt eluents into pure water. With its unique selectivity, researchers have attempted to couple IC with MS for targeted screening and quantification of metabolites such as carbohydrates, organic acids, sugar phosphates, and nucleotides in biological samples.[25−27] Nevertheless, its application in

Received: March 10, 2014
Accepted: April 26, 2014
Published: April 26, 2014

   dx.doi.org/10.1021/ac500951v | *Anal. Chem.* 2014, 86, 5116−5124

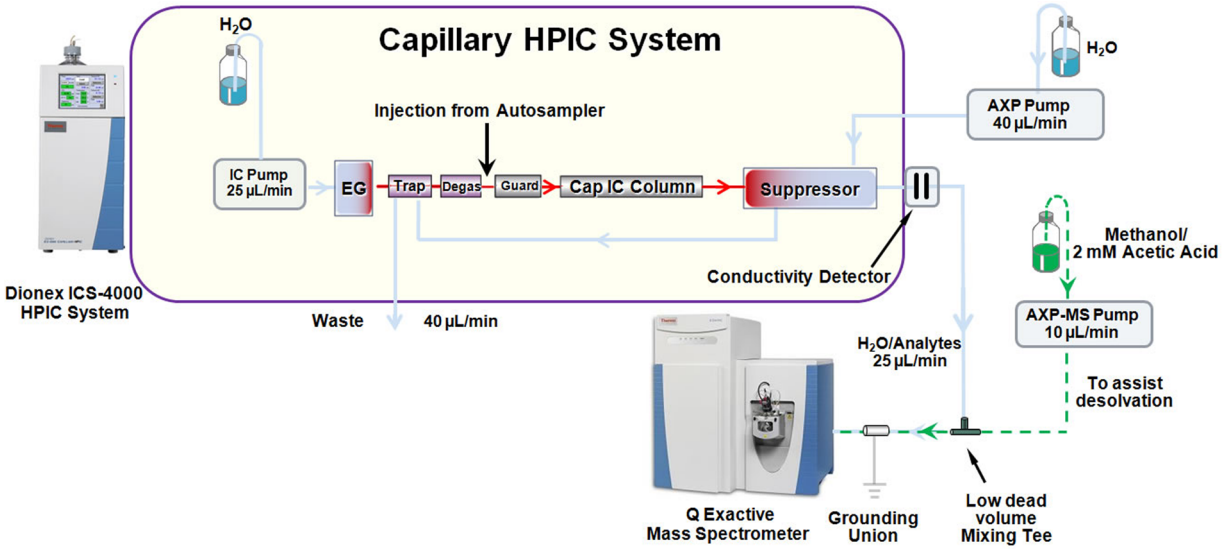

Figure 1. Schematic diagram of capillary ion chromatography-Orbitrap Q Exactive MS system.

untargeted metabolomics has not yet been fully explored. Especially, IC at capillary level flow (5−30 μL/min) is a newly developed platform aiming to improve the sensitivity and applicability in biological analysis.[27] In this study, we coupled the capillary IC (Cap IC) to high-resolution Orbitrap MS in order to achieve a comprehensive untargeted metabolomic analysis.

Head and neck squamous cell carcinoma (HNSCC), including oral SCC, arises from the upper aerodigestive tract (oral cavity, oropharynx, hypopharynx, and larynx) and is the sixth most common type of cancer worldwide.[28,29] MS-based metabolomic analysis has recently been demonstrated for metabolite profiling of tissue or body fluid samples from HNSCC patients.[30,31] These studies have led to the discovery of potentially applicable markers for the disease detection or monitoring treatment effects. In particular, by profiling of saliva samples from patients with oral cancer or oral precancer with LC-MS, a panel of salivary metabolites was found to have predictive value in distinguishing oral cancer from the healthy control or oral precancer. These results suggest that metabolomics approach may complement with the clinical detection of OSCC.[32,33] In this study, we have demonstrated a highly efficient Cap IC-MS method for untargeted metabolomics analysis of head and neck cancer cells and stem-like cancer cells. By comparing the metabolomics profiles of oral stem-like cancer cells (CSCs) to nonstem cancer cells (NSCCs), we found the CSCs have a distinct metabolic phenotype from NSCCs. Using the same methodology, we also revealed siRNA knockdown of transcription factor SOX11 significantly altered the metabolomes in head and neck cancer cells.

EXPERIMENTAL SECTION

Standards. Forty-two polar metabolite standards (Supporting Information, Table S1) were obtained from Sigma-Aldrich (St. Louis, MO). Stock solutions were prepared at 1 ppm (1 μg/mL) in water and stored in −20 °C. The standard mixture was mixed at an equal volume and diluted in series into desired concentrations. A 17 amino acid mixture at 2.5 μmol/mL, referred to as "amino acid Standard H", was obtained from Thermo Scientific Pierce (Rockford, IL) to evaluate the LC methods as described below. For both standard mixtures, water or water/organic solvent were used at a final dilution step according to different chromatography methods.

Cell Culture and Sample Preparation. A spherogenic assay was used to enrich and isolate stem-like cancer cells, as described previously.[34] UM1 cells were initially cultured in DMEM with 10% fetal bovine serum and 1% penicillin/streptomycin (Invitrogen, Carlsbad, CA) and maintained at 37 °C in humidified atmosphere of 5% CO_2. When the cells reached the confluence of ∼90%, the culture media was changed to serum free media (DMEM) containing 1% penicillin/streptomycin and growth factors bFGF (10 ng/mL) and EGF (10 ng/mL) (Geminni Bio, Sacramento, CA). Spherogenic (CSC-like) and nonspherogenic (non-CSC) cells were isolated after the cells were maintained in serum free media for 6 weeks. For siRNA knockdown studies, both UM1 and UM5 cell lines were cultured in DMEM with 10% fetal bovine serum and 1% penicillin/streptomycin (Invitrogen, Carlsbad, CA) and maintained at 37 °C in a humidified atmosphere of 5% CO_2. The cancer cells were transfected with siRNA using Lipofectamine (Invitrogen, Carlsbad, CA) according to the company's instructions. Validated double-stranded siRNAs of SOX11 or nontarget control siRNAs (Santa Cruz Biotech, Santa Cruz, CA) were mixed with the transfection reagent and then added to the cell culture. After a 24 h treatment, the siRNAs were removed, and the cells were further cultured in fresh complete media for 48 h.

Extraction of metabolites was performed according to a previously reported method.[35] Briefly, the cells were quickly washed twice with ice-cold buffered saline solution (PBS) in a cold room to remove medium components and then quickly rinsed with Milli-Q water. After removal of Milli-Q water, the cells were flash frozen with liquid N_2, and 1.0 mL of ice cold 90% MeOH; $CHCl_3$ was immediately added to each plate, and cells were scraped/suspended with a cell scraper. Extracts were transferred to microcentrifuge tubes and pelleted at 4 °C for 3 min at 16 100g. Supernatants were then transferred to new microcentrifuge tubes for LC-MS analysis. All experiments were performed in triplicate.

Chromatography. Five methods were evaluated, including (A) Cap IC running at 25 μL/min (plus 10 μL/min makeup

dx.doi.org/10.1021/ac500951v | Anal. Chem. 2014, 86, 5116−5124

Table 1. Twenty-One Metabolite Standards Used in Figure 2 and Their LODs by Cap IC-Q Exactive MS

peak no.	metabolite name	formula	M−H	on column amount (fmol)	LOD (S/N = 3, nM)
1	D-glucose	$C_6H_{12}O_6$	179.0561	0.17	0.3
2	mevalonate	$C_6H_{12}O_4$	147.0663	2.0	0.1
3	lactate	$C_3H_6O_3$	89.0244	3.4	0.1
4	uridine	$C_9H_{12}N_2O_6$	243.0623	1.2	0.25
5	α-D-glucose 1-phosphate	$C_6H_{13}O_9P$	259.0224	1.2	0.2
6	α-D-glucose 6-phosphate	$C_6H_{13}O_9P$	259.0224	1.2	0.2
7	D-fructose 6-phosphate	$C_6H_{13}O_9P$	259.0224	1.2	0.2
8	adenosine 3′-5′-cyclic monophosphate (cAMP)	$C_{10}H_{12}N_5O_6P$	328.0452	0.91	0.2
9	tartrate	$C_4H_6O_6$	149.0092	2.0	0.5
10	2-oxoglutarate	$C_5H_6O_5$	145.0142	2.1	0.2
11	adenosine 5′-monophosphate (AMP)	$C_{10}H_{14}N_5O_7P$	346.0558	0.87	0.1
12	2-phosphoglycerate	$C_3H_7O_7P$	184.9857	1.6	0.3
13	citrate	$C_6H_8O_7$	191.0197	1.6	0.2
14	isocitrate	$C_6H_8O_7$	191.0197	1.6	0.05
15	*cis*-aconitate	$C_6H_6O_6$	173.0092	1.7	0.2
16	*trans*-aconitate	$C_6H_6O_6$	173.0092	1.7	0.2
17	phosphoenolpyruvate	$C_3H_5O_6P$	166.9751	1.8	0.2
18	D-fructose-1,6-diphosphate	$C_6H_{14}O_{12}P_2$	338.9888	0.88	0.1
19	D-fructose-2,6-diphosphate	$C_6H_{14}O_{12}P_2$	338.9888	0.88	0.1
20	dihydroxy acetone-phosphate	$C_3H_7O_6P$	168.9908	1.8	0.04
21	inosine 5′-monophosphate (IMP)	$C_{10}H_{13}N_4O_8P$	347.0398	0.87	0.1

flow), (B) UHPLC running at 450 μL/min using Hypersil GOLD, C_{18} column, (C) Cap LC running at 40 μL/min using Hypersil GOLD, C_{18} column, (D) HILIC running at 250 μL/min using Merk ZIC-pHILIC column, and (E) Cap HILIC running at 35 μL/min using Phenomenex Luna amine column. Capillary flow HILIC and LC chromatography were performed on a Thermo Scientific Dionex UltiMate 3000 RSLCnano system installed with nanoViper. High-flow HILIC and UHPLC chromatography were performed on a Thermo Scientific UltiMate Dionex 3000 RSLC HPG system.

Cap IC (Method A). A Thermo Scientific Dionex ICS-4000 capillary IC system consisting of a capillary pump, an eluent generator (EG) with a capillary KOH cartridge, and a detection compartment (DC) featuring a capillary IC module with suppressed conductivity detection was used in this study (see Figure 1). The whole system is metal free. The ACES 300 suppressor was operated in external-water mode with ultrapure water (EMD Millipore, Billerica, MA), and regenerant was delivered by an external AXP pump at a flow rate of 40 μL/min. The eluent of the IC system was converted to pure water after the column and was connected to a divert valve that directs the flow to the MS source. To assist the desolvation for better electrospray, makeup solvent MeOH containing 2 mM acidic acid was delivered by an external AXP-MS pump at 10 μL/min and combined with the eluent via a low dead volume mixing tee, and passed through a grounding union before entering the MS. The Cap IC analysis was performed with the IonPac AS11HC-4 μm, 0.4 × 250 mm columns (2000 Å). IC flow rate was 25 μL/min (at 35 °C) supplemented postcolumn with makeup flow. The gradient conditions are as follows: started with an initial 2 mM KOH, increased to 12 mM at 13.5 min, then to 20 mM at 22.5 min and 70 mM at 31.5 min, held 70 mM for 6 min, followed by a decrease to 2 mM within 0.1 min, and held for 7.5 min to re-equilibrate the column. The total run time was 45 min.

LC Methods (Methods B−E). Details were shown in Supporting Information.

Mass Spectrometry. A Thermo Scientific Orbitrap mass spectrometer Q Exactive was operated under ESI negative mode for all detections. Full mass scan (m/z 67−1000) used resolution 70 000 with automatic gain control (AGC) target of 1×10^6 ions and a maximum ion injection time (IT) of 50 ms. Under resolution 70 000, Q Exactive obtains ∼3.5 scan/second full mass scan, or 70 scans cross a Cap IC peak with an average peak width of 20 s, which provides sufficient points for quantitative measurement. Data-dependent MS/MS were acquired on a "Top10" data-dependent mode. Targeted MS/MS was acquired by including the target list. More detailed parameters were shown in Supporting Information.

Data Analysis. Differential analyses of all cell line data were performed using the Thermo Scientific SIEVE 2.1 software, which does background subtraction, component detection, peak alignment, and differential analysis. Statistical results, putative IDs, and pathways were generated by searching ChemSpider and KEGG. The optimized SIEVE parameters for Cap IC were shown in Figure S1. Metabolites of interest were first seared in Metlin using the observed m/z with mass error constraint of 3 ppm at negative mode. Then, the identities were putatively assigned according to MS/MS spectral match to Metlin entries having the MS/MS spectra. The Thermo raw data were converted to mzXML format using ProteoWizard and analyzed by XCMS Online[36] and metaXCMS.[37]

RESULTS AND DISCUSSION

Cap IC/MS Analysis of Metabolite Standards. The MS conditions, Cap IC/MS interface, and autosampler loop setting were optimized for superior sensitivity and minimal sample consumption. Details were shown in Supporting Information.

Forty-two polar metabolites (Table S1) were used to evaluate the analytical performance of Cap IC/MS. The metabolites at a concentration of 60 ppb (0.2−0.7 μmol/L) were detected at signal-to-noise ratio (S/N) of ∼1000, which equals to 0.5−2.5 picomols on column amount. Half of these metabolites were detected at a very low concentration of 60 ppt (0.2 to 3.4 femtomoles on column) with S/N varying from 3 to

dx.doi.org/10.1021/ac500951v | Anal. Chem. 2014, 86, 5116−5124

20. The limits of detection (LODs) for concentration range from 0.04 to 0.5 nmol/L (Table 1), which are lower than commonly reported LODs for concentration by RP-LC methods. The LODs for mass vary from 0.2 to 3.4 fmol, which are comparable to CE-MS for metabolite analysis. These results demonstrate that our capIC-MS platform has excellent sensitivity for metabolomic analysis.

Cap IC/MS separation on the 21 representative polar metabolites at 600 ppb is shown in Figure 2A. Among those,

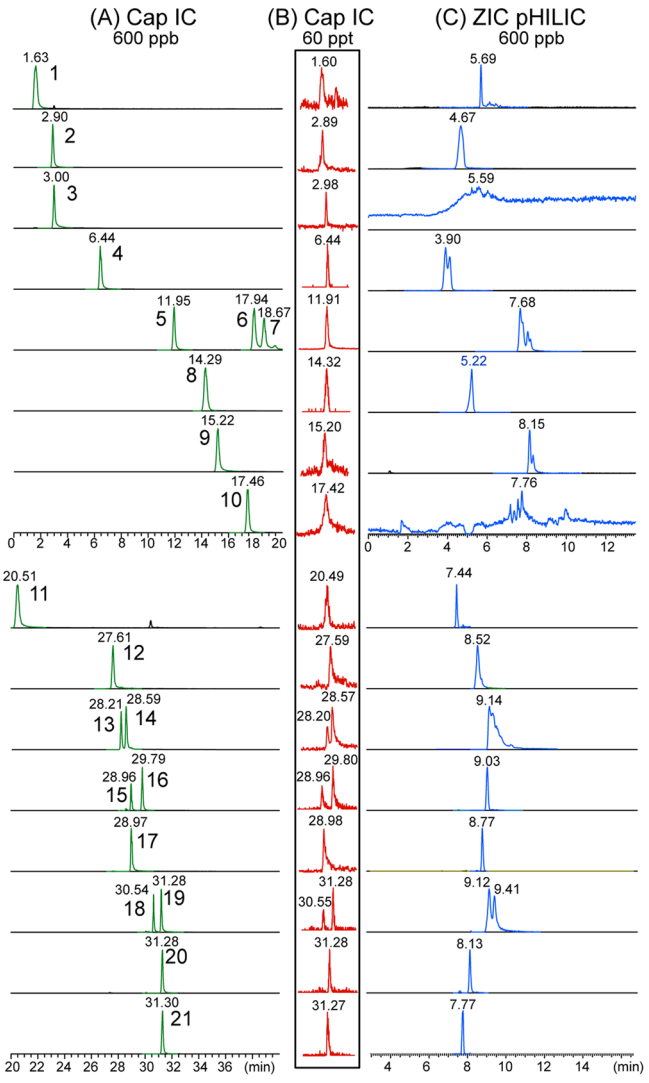

Figure 2. Separation of 21 standard metabsolites at 600 ppb by Cap IC (A), 60 ppt by Cap IC (B), and 600 ppb by HILIC method (C) with Orbitrap MS. Injection volume of 5 μL. Standard mixture for IC was diluted in H_2O and for HILIC was diluted in ACN/H_2O (3:1, v/v). The metabolite IDs are shown in Table 1

four groups of isomeric compounds: (a) α-D-glucose 1-phosphate, α-D-glucose 6-phosphate, and D-fructose 6-phosphate; (b) citrate and isocitrate; (c) *trans*- and *cis*-aconitate; and (d) fructose-1,6-phosphate and fructose-2,6-phosphate had been baseline resolved. The resolution was not affected even when the concentrations were lowered by 10 000-fold to 60 ppt (Figure 2B), and the retention time shifts remained to be less than 0.04 min, demonstrating the IC's good stability and reproducibility over a wide concentration range. To evaluate the interday reproducibility of the Cap IC, analysis was repeated six times within 6 consecutive days. Figure 3 shows the chromatograms using IC conductivity detection on the 42

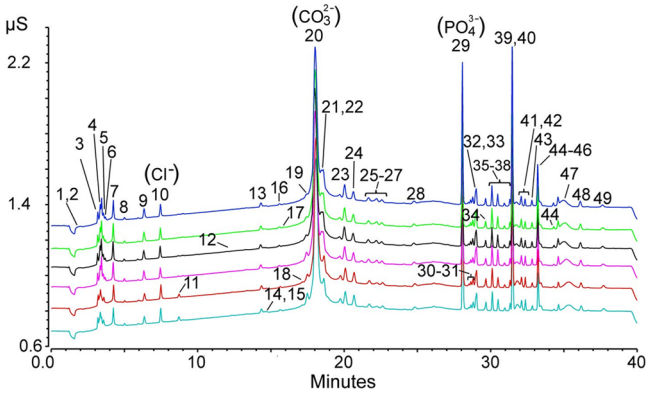

Figure 3. Interday reproducibility analysis of the metabolite standards at 600 ppb by Cap IC with conductive detection (n = 6). Peaks: (1) D-Glucose; (2) D-arabinose; (3) mevalonate; (4) lactate; (5) shikimate; (6) acetoacetate; (7) pyruvate; (8) malate; (9) uridine; (10) chloride; (11) nitrite; (12) glucose 1-phosphate; (13) cAMP; (14) methylmalonate; (15) succinate; (16) tartrate; (17) malonate; (18) 2-oxoglutarate; (19) fructose 6-phosphate; (20) carbonate; (21) maleate; (22) D-glucose-6-phosphate; (23) ribose-5-phosphate; (24) AMP; (25−27) unknown; (28) sulfate; (29) phosphate; (30) citrate; (31) isocitrate; (32) *cis*-aconitate; (33) phosphoenolpyruvate; (34) *trans*-aconitate; (35) ribulose-5-phosphate; (36) D-fructose-1,6-diphosphate; (37) cGMP; (38) D-fructose-2,6-diphosphate; (39) IMP; (40) dihydroxy acetone-phosphate; (41) CTP; (42) ADP; (43) 5-phosphoribosyl-1-diphosphate; (44) ATP; (45) GTP; (46) dGTP; (47) GDP; (48−49) unknown. RSDs of intensity were 5.5%, 7.8%, and 6.0% and RSDs of RT were 6.5%, 8%, and 7.2%, respectively, for the three inorganic ions chloride, carbonate, and phosphate coexisting in the sample solution.

metabolites as mentioned above. Results indicated that the RSDs of intensity and RT for 6 day experiment were within 8%, which is in an acceptable range for relatively quantitative analysis in a metabolomics study.

As a comparison to the IC separation, UHPLC using Hypersil Gold C_{18} RP column and HILIC using ZIC pHILIC column were performed, respectively, with the same Q Exactive MS for detection. C_{18}-based UHPLC separation is one of the most commonly used methods in metabolomics, but how it performs for whole cell metabolites might be of great curiosity. As expected, for the testing polar compounds, the peak shape was mostly unacceptable (data not shown), whereas HILIC showed good separation for most metabolites (Figure 2C). However, the resolution on certain isomers like sugar phosphates and *cis*- and *trans*-aconitate were much worse compared to IC. To validate if the UHPLC and HILIC methods were correctly implemented, the Pierce amino acids standard mixture with a dilution of 1000-fold (5 picomols injected) were analyzed. This is a procedure we have routinely carried out to check system performance in the method development. The results showed good separation and intensity on amino acids (Figure S2), and therefore, the observed results here reflected the true performance of the UHPLC and HILIC methods for those selected polar metabolites. The Cap HILIC and Cap LC to be mentioned below had also been validated, with good separation performance, using this standard mix (Figure S2).

dx.doi.org/10.1021/ac500951v | *Anal. Chem.* 2014, 86, 5116−5124

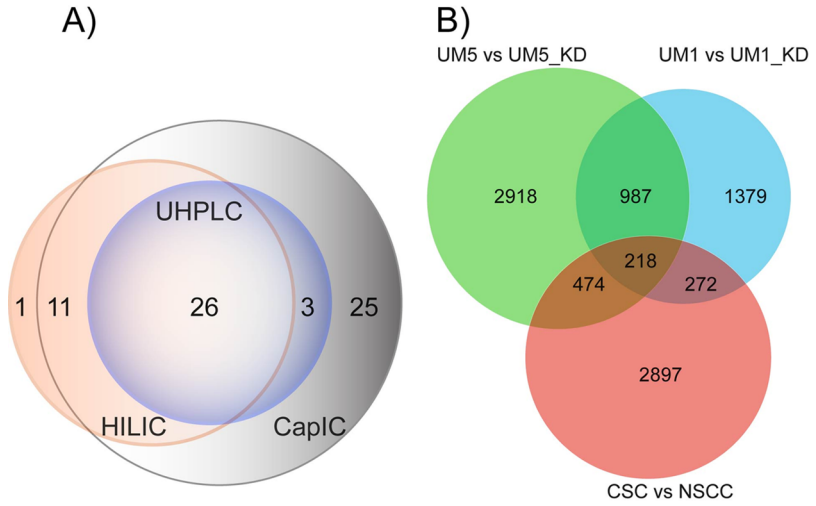

Figure 4. (A) Number of detected peaks corresponding to 42 standards in the UM1 cell lysate obtained by Cap IC and LC methods, (B) the overlap of aligned features among three pairs of cancer cell samples by metaXCMS analysis.

Metabolic Profiling of HNSCC Cells by Cap IC, UHPLC, and HILIC. Before analyzing the cell lysate samples, solvent blank and pool sample were run independently to test the system. Solvent blank was analyzed in full mass scan in order to (1) generate the blank files for post-acquisition background subtraction using SIEVE 2.1 and (2) produce an m/z exclusion list for data-dependent MS/MS experiment. A portion of each cell line lysate sample was pooled to serve as a quality control (QC) sample. The QC sample was run in data-dependent MS/MS mode with exclusion by using the list from solvent blank. For quality control in the data acquisition process, the injections of cell lysate samples were randomized in order to eliminate systematic bias. The cell lysate samples were spiked with 0.5 μmol/L hippuric acid-d5 ($C_9H_4D_5NO_3$), and the pooled sample was intermittently repeated (every 5 runs) throughout the batch analysis. Both were used to monitor the system reliability of intensity and RT. Because many metabolites degraded quickly at ambient temperature, it was critical to reduce the exposure time of the samples in air. Thus, we saved a portion of pooled sample in −80 °C for targeted MS/MS experiment.

In many cases, ionic metabolites like nucleotides, sugars, and so forth, in a synthetic pathway are isobaric isomers, and they play different and important functions in metabolism within the living cells.[38] IC offers an outstanding separation process for the charged and polar compounds. As mentioned above, we used 42 standards, including isomeric compounds (corresponding to 36 m/z values), to evaluate the system performance. The same m/z list was used to extract the peaks from the UM1 cell sample from Cap IC, UHPLC, and HILIC analysis, respectively. As shown in Figure 4A, for this particular m/z list, Cap IC detected 65 peaks (some m/z correspond to multiple peaks), ZIC-pHILIC detected 38 peaks, and UHPLC detected 29 peaks. A total of 26 peaks were detected by all three methods, but obviously Cap IC has a greater coverage. It covered all peaks that could be detected by UHPLC, in which many metabolites were eluted in the dwell volume. Cap IC detected 25 more peaks than HILIC, but only one compound, acetyl-CoA, was detected uniquely by HILIC. This is probably either because the acetyl-CoA molecule is too large for this particular IC column to retain or because the Cap IC mobile phase condition was excessively harsh that it has decomposed during separation. In terms of MS responses, Cap IC and UHPLC showed equivalent or very similar MS intensities and both were 10 to 1000-fold higher than HILIC (Table S1), indicating that the sensitivity loss on HILIC was generally significant.

Among these peaks, remarkably, Cap IC detected 11 peaks at m/z of 259.0225 (Figure 5A). Searching through Metlin library

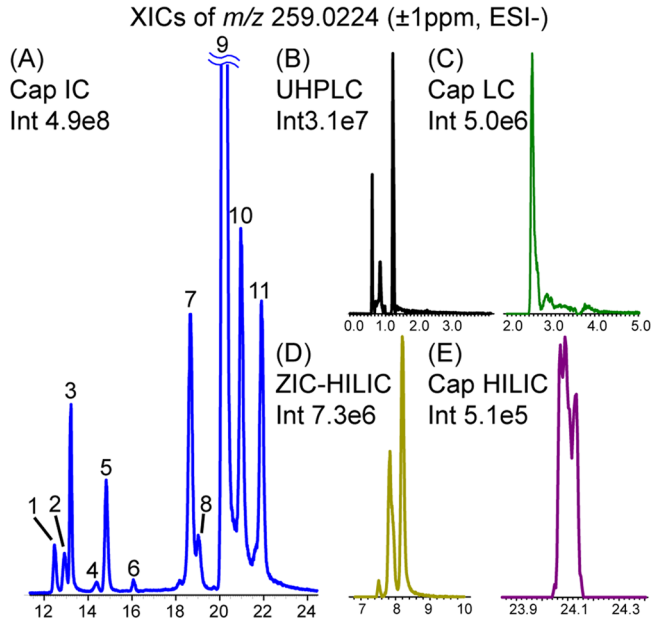

Figure 5. Separation of peaks corresponding to m/z 259.0224 in UM1 oral cancer cells by (A) Cap IC, (B) UHPLC, (C) Cap-LC, (D) ZIC-pHILIC, and (E) Cap-HILIC.

using mass accuracy constraint of 3 ppm for the adduct ions of $[M - H]^-$ and $[M + Cl - H]^-$ returned 33 candidates, all metabolites sharing the formula in the format of $[M - H]^-$ $C_6H_{13}O_9P$. Those candidates include the major and positional isomers of monophosphate conjugating with various sugars like glucose, fructose, galactose, mannose, and myo-inositol, among others. The same peaks from UHPLC and HILIC are shown in Figure 5B,D. The ZIC pHILIC resolved three peaks and appeared to be a satisfactory separation. However, the actual

dx.doi.org/10.1021/ac500951v | Anal. Chem. 2014, 86, 5116−5124

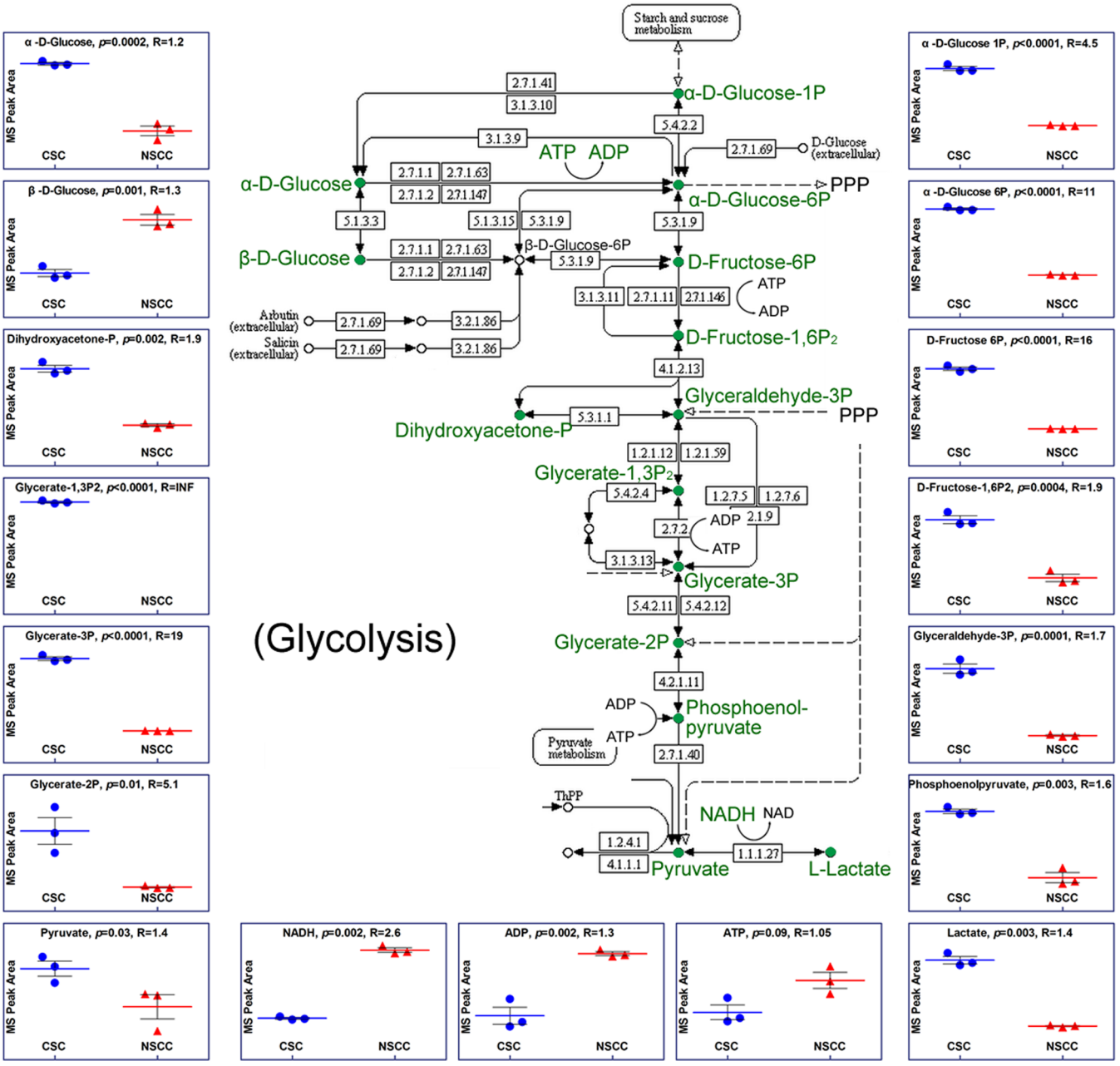

Figure 6. Cap IC/MS analysis revealed metabolic changes of the glycolysis pathway between oral CSCs and NSCCs. *p*: *p*-value; *R*: fold change.

peak number from IC indicated that more than 2/3 of isomeric species were either missing or possibly coeluted in the HILIC separation. Furthermore, to directly compare the sensitivities from a flow rate perspective, Cap LC at 40 μL/min (Figure 5C) and Cap HILIC at 35 μL/min (Figure 5E) were also performed to match the flow rate with Cap IC. However, the mass spectrometric responses for the capillary flow methods were even ~10-fold lower than their high flow versions, and the separations were also worse, implying that the capillary flow LC and HILIC might not necessarily improve the detection of more metabolites. As shown in Figure 5, the intensity loss for the most abundant peak (peak 9 in Cap IC) of the four chromatographic methods, comparing to Cap IC, were 15-fold (UHPLC), 67-fold (ZIC-pHILIC), 100-fold (Cap LC), and 1000-fold (Cap HILIC), respectively.

Differential Analysis, Pathway Mapping, and Meta-Analysis. SIEVE2.1 was used for pairwise differential analysis. We first performed a global metabolomic comparison of UM1 cells versus UM1-KD cells, in which SOX11 was knocked down in the cells. SOX11 is a transcription factor that plays important role in stem cell development and cancer cell progression. However, whether the protein has relevant function in cancer cell metabolism remains unknown. For this sample group, SIEVE detected 1160 components by component extraction (CE), an algorithm that combines multiple ions including monoisotopic peaks, isotopes, adducts, and neutral loss to one master component. This grouping function reduces the effort of mining the large number of detected features or "peaks" during data analysis, tremendously. The component list was then filtered by a combination of *p*-value <0.05 and ratio >2 to refine the targets of interest. In this UM1/UM1-KD sample set, a total of 270 components were found to meet the threshold (*p*-value <0.05 and ratio >2). The filtered data are valuable for expediting the finding of interesting metabolites and altered

dx.doi.org/10.1021/ac500951v | *Anal. Chem.* 2014, 86, 5116−5124

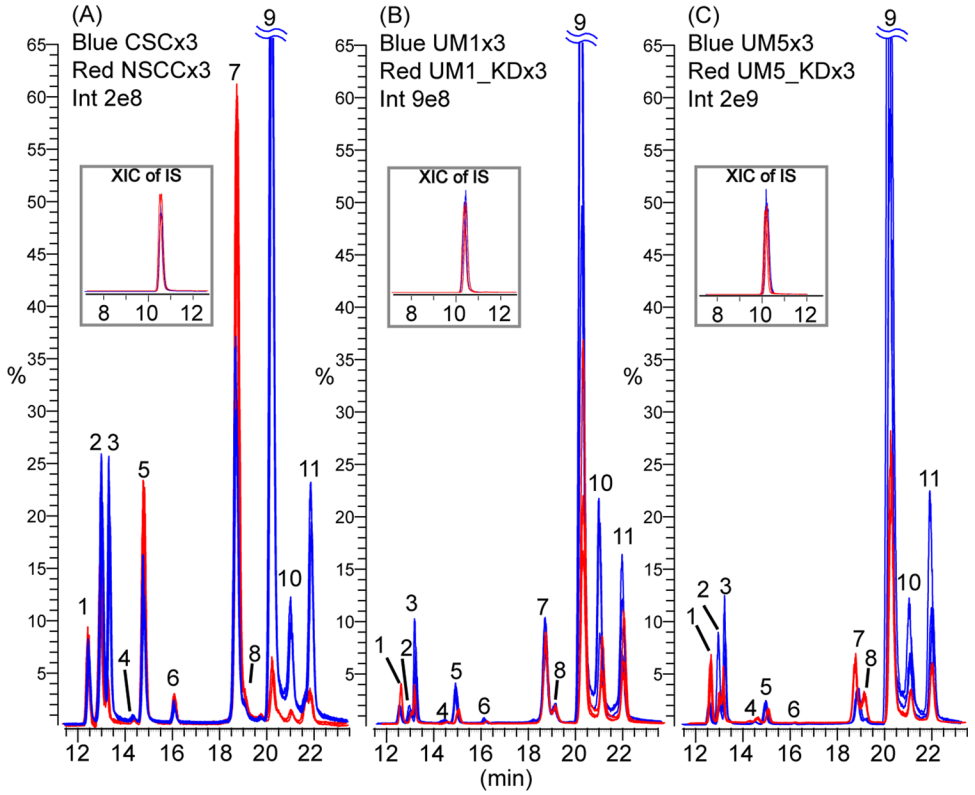

Figure 7. Chromatogram overlays of the 11 sugar monophosphates in three pairs of cancer cell samples. (A) Cancer stem cells (CSCs) versus nonstem cancer cells (NSCCs); (B) UM1 versus UM1-KD; (C) UM5 versus UM5-KD. The insets in each panel are the peak overlays of the internal standard hippuric acid-d5 ($[M - H]^-$183.0824) that was spiked in the cell lysate samples, which showed a very reproducible intensity.

metabolic pathways (as mentioned below); however, a manual analysis is usually conducted to explore the relevant content and to identify possible false positives in terms of identification and quantification. This is probably true to most metabolomics software programs available today, which still need further development to fulfill demanding requests for complicated metabolomics data processing.

Following statistical analysis, mapping of the metabolites to their intrinsic pathways presents an additional important data interpretation step in a metabolomics study by translating the analytical results into biological significance. Many metabolic pathways tools like KEGG, BioCyc, MetaCyc, Reactome, and so forth are available for data mining. After component extraction with SIEVE 2.1, the masses of compounds were automatically searched through KEGG, and matching pathways were displayed. In the UM1/UM1-KD data set, SIEVE found 71 pathways containing between 2 and 36 metabolites. Each pathway includes the component's identification, its name, and related statistic information like maximum change, making data interpretation relatively straightforward. Within these metabolic pathways, glycolysis and tricarboxylic acid (TCA) were altered due to the siRNA-mediated knockdown of SOX11. In our study, we found that knockdown of SOX11 inhibits the proliferation of head and neck cancer cells (data not shown). It seems that down-regulation of SOX11 causes the defects of these metabolic pathways and therefore affects the proliferation rates of these cancer cells. Figure 6 depicts the 17 intermediates of the glycolysis pathway that were detected by Cap IC-MS and their changes between oral CSCs and NSCCs. It is noteworthy that an almost complete coverage of glycolysis metabolites was achieved using the Cap IC-MS method and that the accuracy (RSD < 8%) of the method was sufficient to monitor biologically relevant changes in those metabolite levels. It appears that the level of α-D-glucose was slightly higher (p = 0.0002, fold change = 1.2) in CSCs than NSCCs, as was the level of pyruvate (p = 0.03, fold change = 1.4) and lactate (p = 0.003, fold change = 1.4). In fact, most of the other glycolytic intermediates displayed a significant ($p \leq 0.01$) up-regulation in CSCs compared to NSCCs with fold changes varying from 1.6 to 19, suggesting that the glycolysis pathway has been elevated in CSCs and the dependence of cancer stem cells on the glycolytic pathway has increased compared to nonstem cancer cells. This appears to be a good agreement with the well-known finding that most cancer cells exhibit increased glycolysis.[39] Interestingly, NADH (p = 0.002, fold change = 2.6) and ADP (p = 0.002, fold change = 1.3) levels were down-regulated in CSCs, whereas ATP was not significantly changed (p = 0.09, fold change = 1.05), which confirms activated glycolysis and pyruvate metabolism.

The commonly changed metabolites in all three sample sets (CSC/NSCC, UM1/UM1-KD, UM5/UM5-KD) were of great interest. The metaXCMS software program developed for second-order analysis of global metabolomic data sets was used to perform the meta-analysis.[37] To do so, first, all the three data sets were individually reanalyzed with XCMS Online, which had detected 10 532 (may correspond to 1160 components by SIEVE as described above), 11 377, and 13 302 aligned features for CSC/NCSC, UM1/UM1-KD, and UM5/UM1-KD sample sets, respectively. Then the results were combined and analyzed by metaXCMS. Figure 4B shows the total number of significant features (p-value <0.05, ratio >2) in each sample set and features shared among the samples. A total of 218 features were

dx.doi.org/10.1021/ac500951v | *Anal. Chem.* 2014, 86, 5116−5124

Table 2. Differential Changes of 11 Sugar Monophosphates between Three Pairs of Cellular Samples

				matching		UM1/KD		UM5/KD		CSC/NSCC	
peak no.	obsd $[M-H]^-$	Δ ppm	compound identity	RT	MS/MS	ratio	*p*-value	ratio	*p*-value	ratio	*p*-value
1	259.022 50	0.4	D-myo-inositol (1 or 3)-phosphate	n/a	+	0.49	0.002	0.38	<0.0001	0.98	0.9
2	259.022 50	0.4	unknown	n/a	+	1.7	0.07	1.8	0.46	1.4	0.003
3	259.022 53	0.5	α-D-glucose 1-phosphate	+	+	2.5	0.01	1.8	0.008	4.5	<0.0001
4	259.022 51	0.4	D-myo-inositol (1 or 3)-phosphate	n/a	+	1.5	0.02	0.56	0.04	1.0	0.5
5	259.022 58	0.7	D-mannose 1-phosphate	n/a	+	2.4	<0.0001	1.6	<0.0001	0.67	<0.0001
6	259.022 52	0.5	D-myo-inositol-4-phosphate	n/a	+	2.0	0.003	1.6	0.002	3.0	0.4
7	259.022 60	0.8	α-D-fructose 1-phosphate	+	+	1.1	0.3	0.56	0.0002	0.63	<0.0001
8	259.022 64	0.9	α-D-galatose 1-phosphate	+	+	0.95	0.6	0.15	<0.0001		
9	259.022 61	0.8	D-fructose 6-phosphate	+	+	3.4	0.003	3.9	0.0001	16	0.0002
10	259.022 61	0.8	α-D-glucose 6-phosphate	+	+	3.2	0.001	3.3	0.009	11	0.0006
11	259.022 65	0.9	D-Mannose 6-phosphate	n/a	+	1.8	0.07	2.1	0.004	4.0	0.0006

RT: retention time of the standards; "+" indicates that the RT is available for the standard; "n/a" indicates that the RT is unavailable for the standard.

identified as common to all three sample groups. Figure S3 illustrates the metabolites in the TCA cycle and their differential changes between CSCs and NSCCs. It is very interesting that the first half cycle (pyruvate/citrate/*cis*-aconitate/isocitrate/2-oxoglutarate) had an increasing up-regulation in CSC cells, although the second half cycle (succinate/fumarate/malate) showed progressive down-regulation in CSCs versus NCSC. However, it remains unknown how succinyl-CoA changes between those two cell types. Succinyl-CoA was not detectable by Cap IC, HILIC, or UHPLC in our study, implying that its level might be either too low for the applied methods or the metabolite was not stable under the analytical conditions.

Based on this study, Cap IC/MS detected unexpected large number of sugar phosphate variants, and pathway analysis indicated that those sugar monophosphates had more significant changes than other intermediates in the glycolysis pathway (Figure 6). Figure 7 shows the IC chromatogram overlays of the 11 putative sugar phosphates in the three pairs of cellular samples. Metabolite identification is a key step to biological interpretation and hypothesis generation and it remains a bottleneck in metabolomics analysis today. It is particularly challenging when many isomeric species coexist in a single analysis, as exemplified by the sugar monophosphates detected in this study. To assign the identities for those sugar monophosphates, we acquired the high-resolution MS/MS spectra for the 11 sugar phosphate peaks by targeting *m/z* 259.0224 from the pooled samples (Figure S4). However, two major issues made the identification difficult. First, there is no comprehensive spectral library available containing the complete entry of MS/MS spectra for searching and identification. We compared HMDB, MassBank, NIST, and Metlin and found that only Metlin (http://metlin.scripps.edu/index.php) provided good coverage for those sugar monophosphates. MS/MS spectra of 10 sugar monophosphate isomers in both positive and negative ion mode were previously posted in the Metlin database. Although those fragmentation spectra were acquired through collision-induced dissociation (CID) fragmentation with Q-TOF instruments, all major MS/MS fragments from our data set acquired with the higher energy collisional dissociation (HCD) method in the Orbitrap mass analyzer matched the library spectra very well, as judged by the fragments and their relative abundance. The second reason that is complicating the identification is the finding that the MS/MS spectra for some of the isomers are almost identical, for example, the D-glucose 6-phosphate with D-mannose 6-phosphate, and the α-D-galactose 1-phosphate with α-D-glucose 1-phosphate have the same fragmentation spectrum. To resolve the issue, we compared the retention time (RT) of the peaks identified in our samples against standard compounds. On the basis of matches between the RT and the MS/MS of the standards and our samples, we identified five monophosphate sugar isomers. As indicated in Figure 7, the high-resolution Cap IC separation provided the necessary chromatographic resolution in time to make confident assignments on the basis of the RT of standards. The others were tentatively assigned through the MS/MS pattern match with Metlin (Table 2). Their changes in all cellular samples are summarized in Table 2, and the data indicate that α-D-glucose 1-phosphate (peak 3), D-fructose 6-phosphate (peak 9), α-D-glucose 6-phosphate (peak 10), and D-mannose 6-phosphate (peak 11, tentatively assigned) show consistent changes between UM1/UM1-KD and UM5/UM5-KD samples. These sugar monophosphates were also significantly higher in CSCs versus NSCCs, indicating that the increased levels of monophosphate sugars are common to cancer cells studied in this paper. In particular, D-fructose 6-phosphate and α-D-glucose 6-phosphate showed higher levels (fold change of 11 and 16, respectively) in the CSCs, again implying that glycolysis pathway may be activated in the CSCs.

CONCLUSIONS

We have demonstrated the superior resolution and sensitivity of Cap IC for a challenging analysis of polar metabolites in complex biological matrices such as head and neck cancer cells. Valuable findings regarding the metabolic reprogramming in the sugar metabolism of cancer cells are made possible by the application of IC-HR/AM MS-based methods. In-depth integration of metabolomics with proteomics and genomic data is being carried out in subsequent studies, which may lead to insightful understanding of HNSCC cells, particularly the CSCs. As an emerging analytical tool, the development of a higher-capacity suppressor, new columns for high-throughput analysis, as well as new stationary chemistry for more diverse and larger molecules analysis could be implemented in Cap IC-MS to achieve broader applications in the metabolomics field.

ASSOCIATED CONTENT

Supporting Information

Additional information as noted in the text. This material is available free of charge via the Internet at http://pubs.acs.org.

dx.doi.org/10.1021/ac500951v | *Anal. Chem.* 2014, 86, 5116−5124

AUTHOR INFORMATION

Corresponding Authors

*E-mail: (S.H.) shenhu@ucla.edu. Fax: (310) 794-7109. Tel.: (310) 206-8834.

*E-mail: (Y.H.) yingying.huang@thermofisher.com. Fax: (408) 965-6113. Tel.: (408) 965-6000.

Notes

The authors declare no competing financial interest.

ACKNOWLEDGMENTS

We thank Jessica Wang for the help in microflow LC experiment, Mark Szewc for providing optimized ZIC-pHILIC method, and Linda Lin, Jennifer Sutton, and Ralf Tautenhahn for the help with data processing using SIEVE. Lastly, we thank the University of California Cancer Research Coordinating Committee for funding support (to S.H.).

REFERENCES

(1) Lv, H. *Mass Spectrom. Rev.* **2013**, *32*, 118−128.

(2) Patti, G. J.; Yanes, O.; Siuzdak, G. *Nat. Rev. Mol. Cell. Biol.* **2012**, *13*, 263−269.

(3) Patti, G. J. *J. Sep. Sci.* **2011**, *34*, 3460−3469.

(4) Kuehnbaum, N. L.; Britz-McKibbin, P. *Chem. Rev.* **2013**, *113*, 2437−2468.

(5) Viant, M. R.; Rosenblum, E. S.; Tjeerdema, R. S. *Environ. Sci. Technol.* **2003**, *37*, 4982−4989.

(6) Robinette, S. L.; Brüschweiler, R.; Schroeder, F. C.; Edison, A. S. *Acc. Chem. Res.* **2012**, *45*, 288−297.

(7) Dunn, W. B.; Broadhurst, D. I.; Atherton, H. J.; Goodacre, R.; Griffin, J. L. *Chem. Soc. Rev.* **2011**, *40*, 387−426.

(8) Soga, T.; Ohashi, Y.; Ueno, Y.; Naraoka, H.; Tomita, M.; Nishioka, T. *J. Proteome Res.* **2003**, *2*, 488−494.

(9) Ramautar, R.; Mayboroda, O. A.; Somsen, G. W.; de Jong, G. J. *Electrophoresis* **2011**, *32*, 52−65.

(10) Nemes, P.; Rubakhin, S. S.; Aerts, J. T.; Sweedler, J. V. *Nat. Protoc.* **2013**, *8*, 783−799.

(11) Dunn, W. B.; Knowles, J. D.; Broadhurst, D.; Williams, R.; Ashworth, J. J.; Cameron, M.; Kell, D. B. *Anal. Chem.* **2006**, *79*, 464−476.

(12) Kind, T.; Wohlgemuth, G.; Lee, D. Y.; Lu, Y.; Palazoglu, M.; Shahbaz, S.; Fiehn, O. *Anal. Chem.* **2009**, *81*, 10038−10048.

(13) Saghatelian, A.; Trauger, S. A.; Want, E. J.; Hawkins, E. G.; Siuzdak, G.; Cravatt, B. F. *Biochemistry* **2004**, *43*, 14332−14339.

(14) Gika, H. G.; Theodoridis, G. A.; Plumb, R. S.; Wilson, I. D. *J. Pharm. Biomed. Anal.* **2014**, *87*, 12−25.

(15) Theodoridis, G. A.; Gika, H. G.; Want, E. J.; Wilson, I. D. *Anal. Chim. Acta* **2012**, *711*, 7−16.

(16) Knee, J. M.; Rzezniczak, T. Z.; Barsch, A.; Guo, K. Z.; Merritt, T. J. S. *J. Chromatogr. B* **2013**, *936*, 63−73.

(17) Kiefer, P.; Delmotte, N. l.; Vorholt, J. A. *Anal. Chem.* **2010**, *83*, 850−855.

(18) Cubbon, S.; Antonio, C.; Wilson, J.; Thomas-Oates, J. *Mass Spectrom. Rev.* **2010**, *29*, 671−684.

(19) Creek, D. J.; Jankevics, A.; Breitling, R.; Watson, D. G.; Barrett, M. P.; Burgess, K. E. V. *Anal. Chem.* **2011**, *83*, 8703−8710.

(20) Fritz, J. S. *J. Chromatogr. A* **2005**, *1085*, 8−17.

(21) Bauer, K.-H.; Knepper, T. P.; Maes, A.; Schatz, V.; Voihsel, M. *J. Chromatogr. A* **1999**, *837*, 117−128.

(22) Mohsin, S. B. *J. Chromatogr. A* **2000**, *884*, 23−30.

(23) Conboy, J. J.; Henion, J. D.; Martin, M. W.; Zweigenbaum, J. A. *Anal. Chem.* **1990**, *62*, 800−807.

(24) Mathew, J.; Gandhi, J.; Hedrick, J. *J. Chromatogr. A* **2005**, *1085*, 54−59.

(25) Bruggink, C.; Maurer, R.; Herrmann, H.; Cavalli, S.; Hoefler, F. *J. Chromatogr. A* **2005**, *1085*, 104−109.

(26) Burgess, K.; Creek, D.; Dewsbury, P.; Cook, K.; Barrett, M. P. *Rapid Commun. Mass Spectrom.* **2011**, *25*, 3447−3452.

(27) Wang, L. J.; Schnute, W. C. *Pittcon* **2012**, 1730−13 P.

(28) Kamangar, F.; Dores, G. M.; Anderson, W. F. *J. Clin. Oncol.* **2006**, *24*, 2137−2150.

(29) Chung, C. H.; Parker, J. S.; Karaca, G.; Wu, J.; Funkhouser, W. K.; Moore, D.; Butterfoss, D.; Xiang, D.; Zanation, A.; Yin, X.; Shockley, W. W.; Weissler, M. C.; Dressler, L. G.; Shores, C. G.; Yarbrough, W. G.; Perou, C. M. *Cancer Cell* **2004**, *5*, 489−500.

(30) Yonezawa, K.; Nishiumii, S.; Kitamoto-Matsuda, J.; Fujita, T.; Morimoto, K.; Yamashita, D.; Saito, M.; Otsuki, N.; Irino, Y.; Shinohara, M.; Yoshida, M.; Nibu, K. *Cancer Genomics Proteomics* **2013**, *10*, 233−238.

(31) Ye, G.; Liu, Y.; Yin, P.; Zeng, Z.; Huang, Q.; Kong, H.; Lu, X.; Zhong, L.; Zhang, Z.; Xu, G. *J. Proteome Res.* **2014**, *13*, 1994−2004.

(32) Wei, J.; Xie, G.; Zhou, Z.; Shi, P.; Qiu, Y.; Zheng, X.; Chen, T.; Su, M.; Zhao, A.; Jia, W. *Int. J. Cancer* **2011**, *129*, 2207−2217.

(33) Xie, G.; Chen, T.; Qiu, Y.; Shi, P.; Zheng, X.; Su, M.; Zhao, A.; Zhou, Z.; Jia, W. *Metabolomics* **2012**, *8*, 220−231.

(34) Misuno, K.; Liu, X.; Feng, S.; Hu, S. *Stem Cell Res. Ther.* **2013**, *4*, 156−168.

(35) Lorenz, M. A.; Burant, C. F.; Kennedy, R. T. *Anal. Chem.* **2011**, *83*, 3406−3414.

(36) Tautenhahn, R.; Patti, G. J.; Rinehart, D.; Siuzdak, G. *Anal. Chem.* **2012**, *84*, 5035−5039.

(37) Tautenhahn, R.; Patti, G. J.; Kalisiak, E.; Miyamoto, T.; Schmidt, M.; Lo, F. Y.; McBee, J.; Baliga, N. S.; Siuzdak, G. *Anal. Chem.* **2011**, *83*, 696−700.

(38) Voet, D.; Voet, J. *Biochemistry*, 3rd ed.; John Wiley & Sons, Inc.: New York, 2004.

(39) Pelicano, H.; Martin, D. S.; Xu, R. H.; Huang, P. *Oncogene* **2006**, *25*, 4633−4646.